


AN INNOVATIVE SYNTHESIS OF NANO-ZSM-5 ZEOLITE THROUGH INTERRUPTED ULTRASOUND

<https://scimatic.org/journals/1> 2651-4338

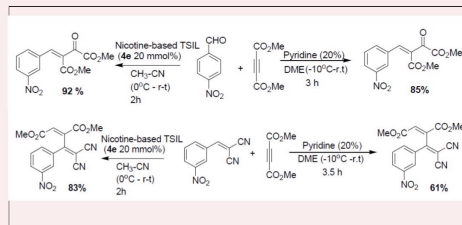
JOURNAL OF ONGOING CHEMICAL RESEARCH

Encouraging Young Chemists

A tidy laboratory means a lazy chemist.
— Jöns Jacob Berzelius (Swedish chemist, 1779–1848)



Volume 1, issue 1, pages 1-44



SciMatic - Scientific Writings and Softwares

JOURNAL OF ONGOING CHEMICAL RESEARCH

2021

Volume: 6

Issue: 1

Pages: 15-23

Document ID: 2021JOCR55

DOI: 10.5281/zenodo.5564497

Manuscript Submitted: 2021-10-12 13:30:16

Manuscript Accepted: 2021-10-12 13:30:32

An Innovative Synthesis of Nano-ZSM-5 Zeolite Through Interrupted Ultrasound

Pirzada Afridi, Farrukh Arsalan Siddiqui*, Sergio Gonzalez-Cortes, Liam France

[For affiliations and correspondence, see the last page.](#)

Abstract

NanoZSM-5 was synthesized with crystal size ≤ 30 nm by using an interrupted ultrasound crystallization process. In his process, the hydrothermal treatment was interrupted with ultrasound and without ultrasound at 170 °C for 24 hours. The nanoZSM-5 crystallinity was confirmed by X-ray diffraction. The crystallite size and morphology were determined by TEM and SEM. The textural properties were investigated by N_2 physisorption. ^{29}Si MAS NMR confirmed the framework composition and presence of silanol group at the surface of the nanoZSM-5.

Keywords: Zeolite, Hydrothermal Treatment, Nano-ZSM-5, Interrupted Ultrasound, Physisorption

INTRODUCTION

Zeolites are microporous crystalline material formed by tetrahedral coordination of heteroatom's (primary Al and Si) linked via oxygen atoms and formed a framework, which composed of cavities and channels where cations, water or other small molecules may reside [1]. ZSM-5 is constructed from several five membered rings called pentasil units. These pentasil units are connected to each other via oxygen to form pentasil chains. In each of the five membered rings, Al and Si are linked together through oxygen atom [1-3] as shown in the Figure 1.

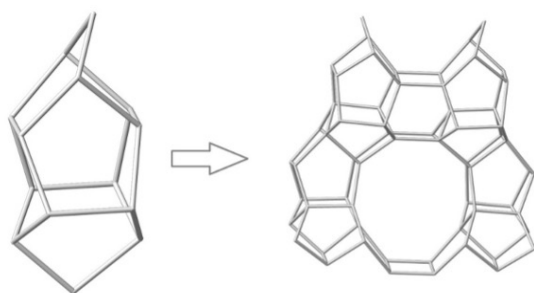


Figure 1. Systematic Structure mechanism of pentasil units connectivity of ZSM-5

According to crystallography the unit cell of ZSM-5 is composed of 96 (Si or Al) T sites & 92 oxygen atom sites. The number of extra framework cations in the unit cell depends on the Si/Al ratio which ranges from 12 to ∞ . ZSM-5 has an orthorhombic unit cell [2,3]. The zeolites acts as a molecular sieves and micropores are of molecular size < 2 nm, it maybe microporous, mesoporous or macroporous materials [4], through which catalytic reactions, adsorption and ion exchange

properties of highly important in the chemical industries [5]. The enhancement of known applications and the possibility of new ones are a keeping main effect to research the tendency to produce zeolites with new order of properties. The effectiveness of the zeolite as catalyst is identified with their morphological and specific properties (well-define crystalline structure, high internal surface area, uniform within the micropore framework [6].

Zeolites have been used as industrial catalysts in many petrochemical processes (e.g., catalytic cracking, hydrocracking, isomerisation, disproportionate, aromatics alkylation, methanol to gasoline, dewaxing) [1]. During the industrial processes most of the zeolites based catalyst are frequently deactivated because of the coke formation in the process [7,8]. Nanocrystalline zeolite have larger surface area as compared to micron size zeolites; therefore, nanocrystalline zeolites have good accessibility to the internal micropores, which may influence the catalysis and adsorption properties. e.g., Due to the smaller diffusion path shown slower the deactivation rate of the catalyst [4,9,10]. The nano-size zeolites have significant effect on diffusion rate and the reaction rate, which greatly improve the catalytic activity. Recently nano-size ZSM-5 attracted by the researchers due to its great performance using as a catalyst, such as shape selective, high steam stability, high metal resistance and lower coke production [11,12].

The researchers digging various different paths to synthesized nano-size ZSM-5 crystals have been produced. The method of the crystallization process also the morphology and particular properties (crystal size and distribution) of ZSM-5 zeolite are impact by distinctive variables: the aluminium content, silicon and aluminium sources, the nature of cations present in

the synthesis medium, alkalinity, temperature of the crystallisation, seeding method, water content [13].

Ultrasound is an important phenomenon not only used for the medical purposes but also to affect the distribution of crystallite size and crystal growth in the crystallization process [14]. Initially in the syntheses of zeolites, the alkaline aluminosilicate gel is normally aged in order to obtain the smallest crystallite size and to improve the product [15]. Therefore, to enhance the nucleation and to get the required crystallite size different modes of aging are used. Aging with ultrasound has been a powerful tool for the enhanced nucleation process in liquid/gel based solutions [16,17]. In this work, ultrasound was used at different stages in aging/pre-treatment and interrupted crystallization in order to enhance the nucleation process to achieve the nano scale particles/crystals of the ZSM-5 zeolite.

Nucleation is a phenomenon in which the “nucleus” typically a small seed crystal or dust particle in the amorphous phase of a solution initiates crystallisation. Nucleation is the first step of the crystallization process. A significant energy barrier can be overcome at higher level of supersaturation. If supersaturation is very high, higher number of nuclei will be formed [18] as shown in Figure 2 where step III is a supersaturation leading to higher number of nuclei. The rate of nucleation is directly related to concentration and inversely proportional to temperature. The process in which the materials arranged from the solution through a growth process is called crystallization [19].

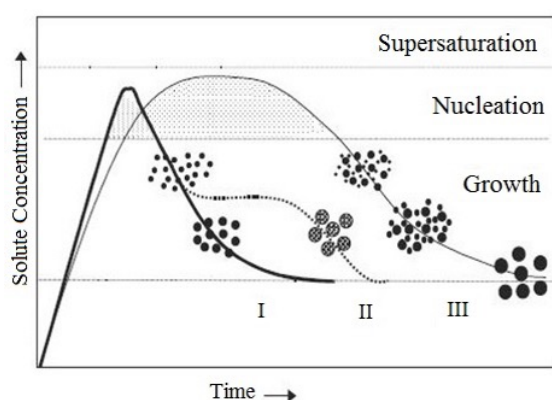


Figure 2. Proposed mechanism of nucleation and crystal growth in supersaturation solution: I) Single nucleation and uniform crystal; II) Nucleation, growth and aggregation of smaller subunits; III) Multiple nucleation events and crystals growth

The zeolite synthesis mechanism consists of complex nucleation and crystal growth. To enhance the

nucleation step of the crystallization mechanism, we studied different aging techniques before hydrothermal treatment, because nucleation occurs during the aging. The inorganic precursor gel produced uniform and highly crystalline material using optimized reaction conditions. A number of different routes for zeolite synthesis mechanism have been proposed. The most prominent issue arising in the discussion of this mechanism was particles aggregation. Therefore, particle aggregation is one of the main focuses of synthetic research in zeolite chemistry. In order to understand the zeolite synthesis and crystal growth mechanism numerous studies have been reported. Sharma et al [20] proposed a successful mechanism starting from primary nanoparticles of gel which then nucleate and end up with cubic crystal aggregates as shown in Figure 3. The primary nanoparticles of the gel can lead to any of the three proposed mechanisms depending on the reaction conditions. Path I describes the conversion of the primary nano particles into crystals after passing through dissolution and monomeric growth. Path II explains the seeding mechanism for the conversion of the primary nano particles to crystals. Path III describes the formation of aggregates of the nano particles, which then convert into a large crystal. Abrishamkar et al [21] reported a zeolite crystallization mechanism using various techniques for enhancing the nucleation period prior to hydrothermal treatment [20].

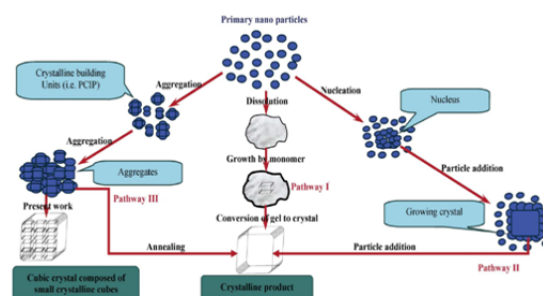


Figure 3. Three different mechanisms representing the zeolite crystal growth. Path I) Considered monomer precursor and the amorphous gel particles maintained average size. Path II) follows by the addition of primary particles and grow the crystals. Path III) large particles were grown from the aggregation of the small particles

In the recent decades synthesis of nanosize crystalline ZSM-5 widely investigated [22,23]. Agglomerates of nano-crystalline silicates have been synthesized rapidly. The solution is concentrated for 10-12 hours of aging at 80 °C, after that passes to hydrothermal treatment for 90 minutes at 170 °C. The powder was then characterized by DLS, XRD and FTIR [24]. Nanocrystalline ZSM-5 was produced by hydrothermal

method for 24 hours using clear supersaturated homogeneous solution. The uses of aluminium source, long aging time, pH, water content and presence of alkaline cations have been investigated to produce nanocrystalline ZSM-5. The product was then characterized by XRD, solid state MAS-NMR, TEM and nitrogen adsorption (BET) in order to examine the crystallisation mechanism [22].

Leached metakaolin has been used to synthesize nanosize ZSM-5 aggregates by solid state conversion. The synthesis was based on the conditions of molar ratios of TPA + /SiO₂, NaOH/SiO₂ and SiO₂ /Al₂O₃ and the final product was examined. The aggregates of nanosize ZSM-5 was then characterised by XRD, SEM, HRTEM, MAS NMR, NH₃-TPD, TG and N₂ adsorption and desorption and particle size analysis. The reports showed that the nanosize ZSM-5 was produced within 2 hours by solid like state conversion. TEM revealed that the ZSM-5 powder aggregates were irregular spheres consist of nano-size crystallite about 30-50 nm [25]. Schmidt et al reported confined space synthesis, which is a new procedure for the synthesis of nanosize zeolite. According to this process crystallization of the zeolite occurs in the pore networks of the mesoporous cages. With the help of this method they synthesised nanosize ZSM-5 and zeolite Beta controlled size distribution. All the samples were characterized by XRD, Transmission electron microscopy and nitrogen adsorption/desorption and the crystallite size reported was 20-75 nm [26].

Based on the observations and thoroughly studying the literature we synthesised nanoZSM-5 50-100 nm, increasing nucleation time. The gel was treated with ultrasound before hydrothermal process. Thus, in this method we successfully reduce the aggregation of particles and the nanoZSM-5 crystallite size. The crystallite powder was then characterized with help of different advanced spectroscopic techniques such as XRD, TEM, DLS and NMR.

RESULTS AND DISCUSSION

Powder X-ray Diffraction (XRD)

Powder X-ray diffraction was used to identify the structural framework of crystalline materials. The crystallite size and the crystallinity of the as synthesized ZSM-5 powder were also calculated from X-ray diffraction patterns.

After the use of ultrasound in pre-treatment of the

hydrothermal process, the ultrasound was used for the first time in the interrupted synthesis in hydrothermal process of nanoZSM-5 zeolite synthesis. Venkatathri [30] reported the interrupted synthesis of ZSM-5 but did not explain the procedure or the mode of interruption during synthesis. Numerous experiments were performed with and without ultrasound interrupted syntheses and also with increasing temperature from 20 to 170 °C during the course of crystallization as shown in Figure 5 (a), (b), (c) and (d). The crystallinity of all the samples was calculated with help of equation (1). The crystallite sizes of all the obtained X-ray diffraction patterns were also calculated using Scherrer's equation.

$$RC = \frac{\sum I_{(high\ crystalline\ peaks)}}{\sum I_{(Reference)}} \times 100\% \quad (1)$$

Where RC is the relative crystallinity and I is the peaks integrated area.

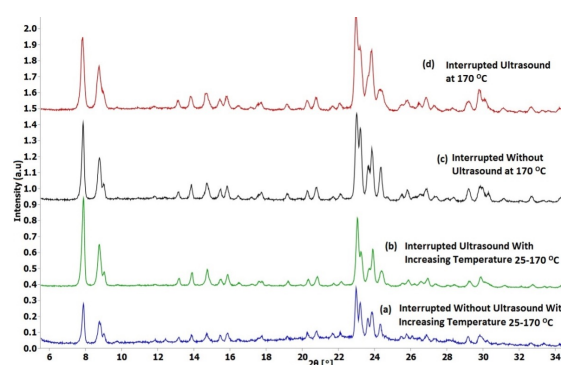


Figure 4. X-ray diffraction of the as synthesized nanoZSM-5 by different methods of interruption using ultrasound and without ultrasound

The calculated data are illustrated in Table 1. The samples (d) and (c) are X-ray powder diffraction patterns of the as synthesized nanoZSM-5 with and without ultrasound interrupting the crystallization process respectively. From the diffraction patterns, the broadening was observed in the Bragg peaks of sample (d) which was synthesized using ultrasound interrupted as compared to the sample (c) which was synthesized without using ultrasound. The calculated crystallite size of both samples was 27±5 nm and 85±5 nm respectively. A significant reduction in the crystallite size was observed by using ultrasound interrupting crystallization process. Variations in the average FWHM of the peaks ranging from 20 to 30° in 2θ are listed in Table 1.

Similarly, the X-ray diffraction pattern of samples (a) and (b) are shown in Figure 5. Sample (a) was treated

without ultrasound, it shows the presence of both crystalline and amorphous phases. Hence, the pattern composed of amorphous phase, so neither crystallinity nor crystallite size was calculated. The X-ray diffraction of the sample (b) shows a pure phase of ZSM-5. The calculated relative crystallinity and the calculated crystallite size are illustrated in Table 1.

Table 1. Average crystallite size and the calculated relative crystallinity for the as synthesized nanoZSM-5 samples by interrupted synthesis with and without ultrasound

Samples	Time of Interrupted modes (min)		Crystallisation Temp (°C)	Ave. FWHM (2θ) (°)	Ave. Cry. Size (nm)	Cryst (%)
	With Ultrasound	Without Ultrasound				
a	-	180	Increased 20 to 170	N.C	N.C	N.C
b	180	-	Increased 20 to 170	0.127±0.05	87±5	40±5
c	-	180	Fixed 170	0.129±0.05	85±5	80±5
d	180	-	Fixed 170	0.345±0.05	27±5	120±5

Transmission Electron Microscopy (TEM)

The crystallite size distribution of the *as synthesized* nanoZSM-5 was studied using high resolution TEM. Figure 6 depicts TEM images of the sample (a), (b), (c) and (d) of nanoZSM-5 synthesized for 24 hours with and without ultrasound interrupted treatment. Samples (a) and (b) shows different particles sizes and have different morphology. X-ray powder diffraction of samples (a) showed the presence of an amorphous phase, while sample (b) was a single ZSM-5 powder diffraction pattern. The sample (a) was not treated with ultrasound for 24 hours with increasing temperature from 20 to 170 °C. During the last 8 hours of the hydrothermal treatment, the temperature was uniform at 170 °C. Some large cookie like morphology crystals were observed at 2 μm (2000 nm) diameter. The sample (b) was synthesized with interrupted ultrasound, with a temperature profile identical to sample (a). A rectangular or brick like aggregated morphology was observed, which is completely different from that of the sample (a). The size of aggregated particles are ~500 nm.

TEM images of the *as synthesized* nanoZSM-5 particles without and with interrupted ultrasound at 170 °C for 24 hours are shown in Figure 6 (c) and (d) respectively. The sample (c) was synthesized without the use of ultrasound but with a static aging interruption for 15 minutes after every 2 hours hydrothermal treatment. The particles has similar morphology as the sample (a), but the recorded particle dimension was ≤400 nm. The sample (d) synthesized with interrupted ultrasound shows an

undefined morphology with very small particles sizes ranging from 10 nm to 30 nm.

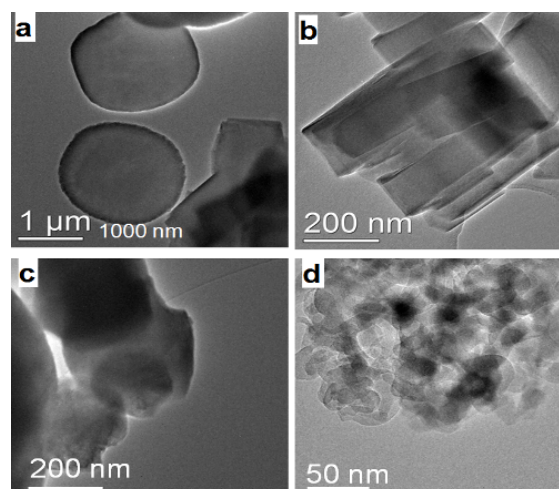


Figure 5. TEM micrographs of the as synthesized samples. a) Interrupted synthesis without ultrasound with increasing temperature from 20 to 170 °C; b) Interrupted synthesis with ultrasound with increasing temperature from 20 to 170 °C; c) Interrupted synthesis without ultrasound at 170 °C; d) Interrupted synthesis with ultrasound at 170 °C

The ultrasound treatment has a remarkable influence on the product phase, including particle size reduction and an enhancement of the crystallinity. By comparing the TEM micrograph of this data with the data reported in the previous chapter close agreement is seen for the effect of ultrasound to produce nanoZSM-5 using different experimental conditions.

Dynamic Light Scattering (DLS)

DLS was used to investigate the particle size distribution of all the *as synthesized* nanoZSM-5 using different preparation methods. Figure 7 (a) and (b) shows the samples prepared without and with ultrasound interrupted synthesis with increasing temperature from 20 to 170 °C for 24 hours respectively. Sample (a) was composed of crystalline and amorphous phases with large aggregations of the particles as determined by X-ray diffraction, TEM and SEM analysis. The average dimension of the particle size observed using DLS was around 1000 nm. Similarly, the observed range of particle size was 400-500 nm for the sample (b). DLS also showed the particles aggregation in the sample (b).

DLS measurements of the samples synthesized with uniform heating at 170 °C without and with interrupted ultrasound treatment are shown in Figure 8 (c) and (d) respectively. The observed average particle size was 400-500 nm for sample (c). While the average

particle size observed of sample (d) was 10-50 nm as shown in Figure 8 (d). This DLS analysis on sample (d) shows a significant effect of the ultrasound and the interruption of the hydrothermal conventional treatment on the particle size distribution in the product zeolite.

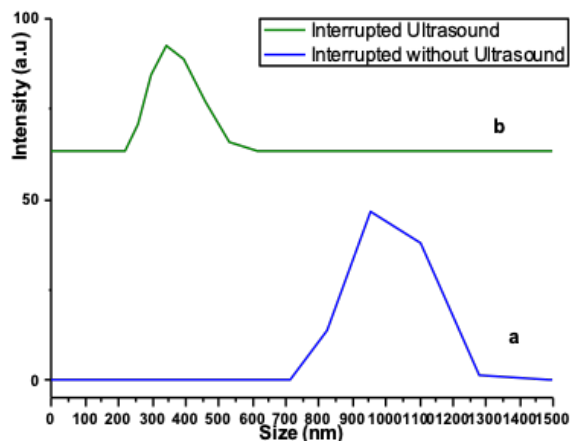


Figure 6. DLS data of the as synthesized micro and nanoZSM-5 samples. a) Interrupted synthesis without ultrasound with increasing temperature from 20 to 170 °C, b) Interrupted synthesis with ultrasound with increasing temperature from 20 to 170 °C

In terms of the average calculation, large crystals predominate in the crystallite size distribution. The X-ray diffraction and TEM results from the synthesized samples give a very close agreement with the data obtained by DLS.^[26,31–33] All the obtained data of the as synthesized data are compared in Table 2.

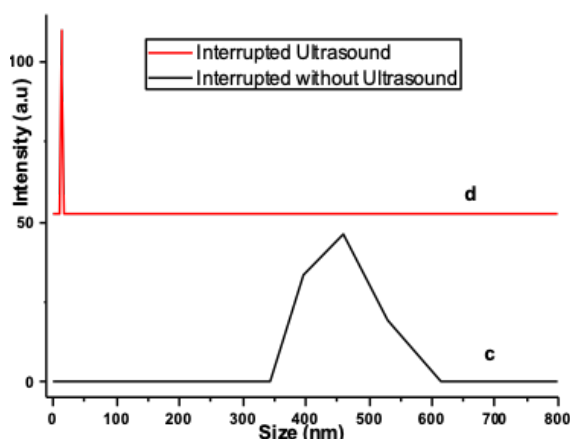


Figure 7. DLS data of the as synthesized micro and nanoZSM-5 samples. c) Interrupted synthesis without ultrasound at 170 °C and d) Interrupted synthesis with ultrasound at 170 °C

Energy-Dispersive Spectroscopy (EDS)

EDS analysis was used to confirm each component of the as synthesized nanoZSM-5. EDS was used on

TEM to obtain the average weight % of each element present in the as synthesized ZSM-5 samples. From the EDS spectra in Figure 9 it can be seen that all the samples are composed of silicon and aluminium oxides, which are the constituent elements (Si, Al and O) of the zeolite framework (ZSM-5). The average weight percent (wt. %) of all the basic elements of the framework are illustrated in Table 3.

Table 2. Comparing the particles size distribution obtained by XRD, TEM, SEM and DLS analysis of the synthesized with and without interrupted ultrasound treatment

Samples	Time of Interrupted modes (min)		Average Particles Size (nm)				Crystallinity (%)
	With Ultrasound	Without Ultrasound	XRD	TEM	SEM	DLS	
A	-	180	N.C	2000	3000	3000-5000	48±5
b	180	-	87±5	~500	800	800-1000	55±5
c	-	180	85±5	400	300-500	500-800	67±5
d	180	-	27±5	10-30	100-200	10-50	82±5

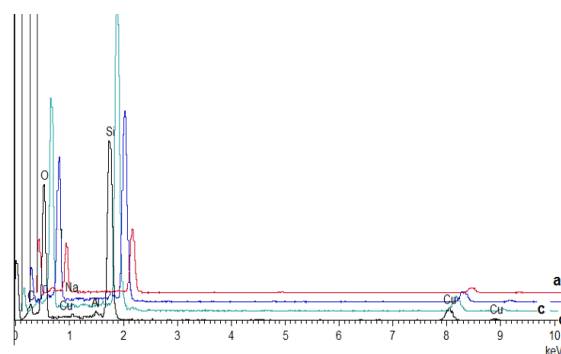


Figure 8. EDS spectra of the as synthesized samples. a) Interrupted synthesis without ultrasound with increasing temperature from 20 to 170 °C, b) Interrupted synthesis with ultrasound with increasing temperature from 20 to 170 °C, c) Interrupted synthesis without ultrasound at 170 °C and d) Interrupted synthesis with ultrasound at 170 °C

These SAR results are similar to the already reported results of the as synthesised ZSM-5 zeolite [34–36]. However, the synthesis mechanism and the pre-treatment methods in this study are different from the literature reports.

Table 3. Chemical composition obtained by EDS analysis of the samples prepared by static with and without interrupted ultrasound synthesis

Sample	Average wt (%) Elemental Composition			Si/Al
	Si	Al	O	
a	21.43	0.53	29.52	40.4
b	22.22	0.63	40.69	35.3
c	21.8	0.68	35.45	32.1
d	22.65	0.59	37.48	38.4

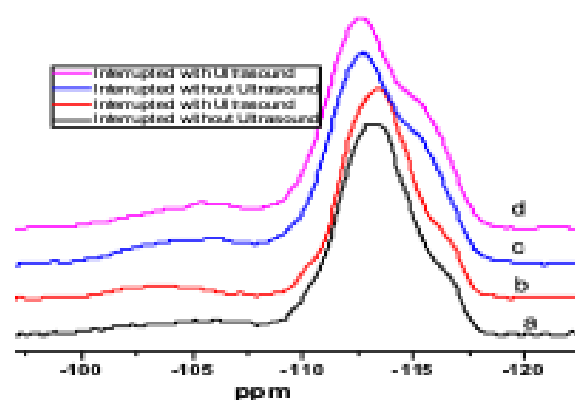
Table 4. Particles size distribution and SAR of the as synthesized nanoZSM-5 samples using ultrasound pre-treatment

Samples	Average Particles Size (nm)				Si/Al (SAR)	Crystallinity (%)
	XRD	TEM	SEM	DLS		
A	N.C	2000	Micro-Nano	1000	40.4	Not calculated
B	87±5	500	300-500	400-500	35.3	40±5
C	85±5	500-800	100-500	400-500	32.1	80±5
D	27±5	10-50	100-200	10-30	38.4	120±5

Solid State Magic Angle Spinning Nuclear Magnetic Resonance (MAS NMR)

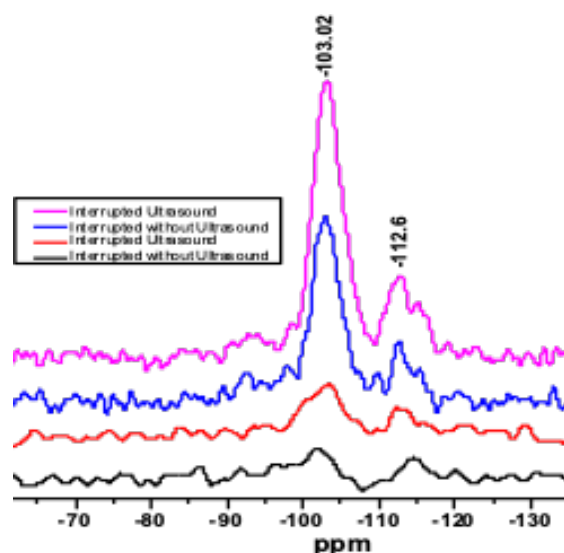
Silicon is in a tetrahedrally coordinated in the framework therefore, it has five different potential environments such as Si(*n*Al) where *n* ($n \leq 4$) is the number of Al atoms connected to silicon via oxygen bridges.

The ^{29}Si MAS NMR spectra of the sample in Figure 10 (a), (b), (c) and (d) are quite similar to those previously reported.^[37,38] ^{29}Si MAS NMR spectra of each include a major chemical shift at -113 ± 1 ppm with an overlapping signal at -115 ± 2 ppm. Those are assigned to Si(*0*Al) coordination in the ZSM-5 framework. There is also a broad resonance from -103 ± 2 to -106 ± 1 which is assigned to Si(*1*Al) for the ZSM-5 framework.^[13,38,39] The chemical shift at -103 ± 2 and -106 ± 1 ppm gives evidence of the presence of silanol group on the surface.^[13,30,37]

**Figure 9.** ^{29}Si spectra of the samples obtained by different synthesis methods. a) Interrupted synthesis without ultrasound with increasing temperature from 20 to 170 °C, b) Interrupted synthesis with ultrasound with increasing temperature from 20 to 170 °C c), Interrupted synthesis without ultrasound at contact temperature at 170 °C and d) Interrupted synthesis with ultrasound at contact temperature at 170 °C

The ^{29}Si MAS NMR spectra was also supported by the $^1\text{H} \rightarrow ^{29}\text{Si}$ cross polarization (CP) MAS NMR spectra as shown in Figure 11 (a), (b), (c) and (d). There are

two main chemical shift values observed at 103 ± 0.5 ppm and 112 ± 1 ppm. These values confirm that the terminal hydroxyl group is directly connected to Si atom in SiO_4 tetrahedron (Si(*1*OH)). The concentration of the silanol group increased with decreasing particle size from sample (a) to (d) from 1000 nm to <50 nm respectively as shown in Figure 11.

**Figure 10.** $^1\text{H} \rightarrow ^{29}\text{Si}$ cross polarization (CP) spectra of the samples obtained by different synthesis methods. a) Interrupted synthesis without ultrasound with increasing temperature from 20 to 170 °C b) Interrupted synthesis with ultrasound with increasing temperature from 20 to 170 °C c) Interrupted synthesis without ultrasound at contact temperature at 170 °C d) Interrupted synthesis with ultrasound at contact temperature at 170 °C

Deconvolutions of all the ^{29}Si MAS NMR spectra are shown in Figure 12 (a), (b), (c) and (d). The sample (a) as explained in the X-ray diffraction section it is composed of crystalline and amorphous phase. The ^{29}Si spectra illustrate that there are ≥ 10 chemical shift peaks observed. Most of the resonance occurs in the range from -110 ppm to -117 ppm. Such kind of ^{29}Si spectra has been reported in the literature but without assigning all the chemical shifts of the spectra.^[39] The spectra of samples (a) were automatically deconvoluted using the VnmrJ NMR software, while the spectra of samples (b), (c) and (d) were deconvoluted manually. Sample (b) has some small roughness in the peak difference line, indicating that there are still some small chemical shifts which are unaccounted for in the deconvolution. On the other hand, samples (c) and (d) as shown in Figure 12 were highly crystalline nanoZSM-5. It was also noticed that the calculated peak over-lap on the experimental peaks of all the samples as shown in Figure 12 (b), (c) and (d), indicating a very fine and precise deconvolution. The increased in the aluminium site in samples (c) and

(d) also may confirm the increased of acidic sites on the surface, as the terminal silanol group increased as the particle size decreased to ≤ 30 nm.

^{27}Al and ^{29}Si MAS NMR spectra confirmed the nanoZSM-5 framework structure. Line width broadening of both the spectra evidenced that the crystallite size decreased. The acidic site increased as the particle size decreased.

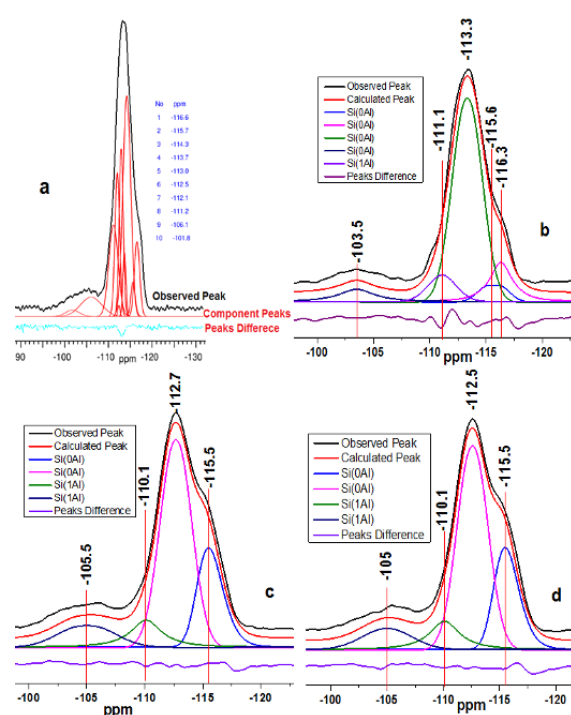


Figure 11. Deconvoluted ^{29}Si spectra of all the samples obtained by different synthesis methods: a) Interrupted synthesis without ultrasound with increasing temperature from 20 to 170 °C; b) Interrupted synthesis with ultrasound with increasing temperature from 20 to 170 °C; c) Interrupted synthesis without ultrasound at contact temperature at 170 °C; d) Interrupted synthesis with ultrasound at contact temperature at 170 °C

EXPERIMENTAL

Synthesis of nanoZSM-5

NanoZSM-5 samples were synthesised from clear gel solution through hydrothermal process after treated with ultrasonication in water bath and static condition of aging. The reaction mixture is composed of the following molar ratio: SiO_2 : NaAlO_2 : NaOH : TPAOH : H_2O plus using Ethanol half of the solution mixture.

The chemical reagents included tetrapropylammonium hydroxide (TPAOH), 40 wt.% from Sigma Aldrich, tetraethyl orthosilicate (TEOS) silica source from

Sigma Aldrich reagent grade 98%, sodium aluminate (NaAlO_2) used as Al source, ca 8% water, 99.9 % Al, supplied from ABCR GmbH & Co.KG, sodium hydroxide (NaOH) analytical reagent from Fisher Scientific UK, was used as alkaline media, Ethanol absolute ≥ 99.9 % from Sigma-Aldrich.

NanoZSM-5 was prepared in alkaline water mixture containing Si and Al source and alkaline metal cation. The organic structure directing agent (which is very important to the zeolite framework formation) was also added to the solution mixture and stirred for 10-20 minutes and at the same time ethanol also added to the mixture which act as a solvent and also help to reduce the aggregation during the crystallization. The mixture is then passed on to the ultrasonication using ultrasound bath for different time intervals. The mixture is then poured into a Teflon-sealed stainless steel autoclave and heated to a desirable temperature for a specified reaction time. The ultra-sonication and heating steps repeated after every 2 hours intervals till to the end of the experiment as shown in Figure 4.

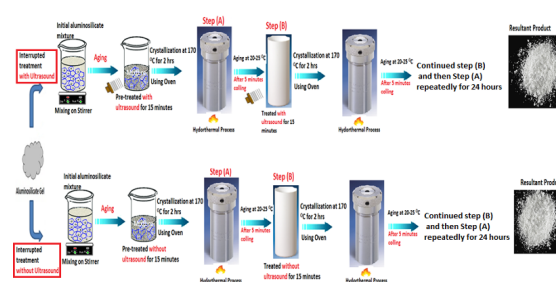


Figure 12. Interrupted synthesis mechanism of nanoZSM-5 using ultrasound

Effect of ultrasound before hydrothermal treatment

The aluminosilicate gel in the beaker was treated with sonic waves using ultrasound bath, which produce mechanical vibration in gel. The vibrations ultimately creating pressure waves in the solution, which produces millions of microscopic bubbles (cavities). When these cavitation bubbles implode it formed high-pressure micro jets and micro streams. This phenomenon is due to implodes process, which is a very fast process. Implodes process is very short as compared to its initiation time. The power of ultrasound and cavitation phenomena is the major contributing factor in the primary nucleating and crystallization process [27–29].

Characterization

X-ray powder diffraction (XRPD)

The Powder pattern of the synthesised nanoZSM-5 was obtained a Philips X'pert X-ray diffractometer with CuK α radiation. Each sample was run for 90 minutes.

Dynamic light scattering (DLS)

The size of the nano-particles obtained after hydrothermal treatment were analysed by a ZetaSizer-300 dynamic light scattering instrument (Malvern, 10mW He-Ne laser and fixed scattering angle of 90 °C).

High-resolution transmission electron microscopy (HRTEM)

High-resolution transmission electron microscopy (HRTEM) was examined on JEOL 2010 analytical, which has a LaB 6 electron gun and can be operated between 80 and 200kV. This instrument has a resolution of 0.19 nm, an electron probe size down to 0.5nm and a maximum specimen tilt of ± 10 degrees along both axes. Samples were dispersed in water and a drop of the dispersion was deposited on a holey carbon coated Cu TEM grid and dried at room temperature for several hours before examination in the TEM.

Solid state magic angle spinning nuclear magnetic resonance (SS MAS NMR)

Direct polarization (DP) magic angle spinning (MAS) nuclear magnetic resonance (NMR) was used to study the local environment of Si, and Al. ^{27}Al solid state MAS NMR spectra were acquired at 52.15 and 200.1 MHz for ^{27}Al and ^1H on a Varian Chemagnetics CMX infinity 200 (4.7 T) spectrometer, using 6 kHz rotation with each spectrum resulted by 100s delay. The ^{27}Al chemical shift were referenced to an aqueous solution of $\text{Al}(\text{NO}_3)_3 = (0 \text{ ppm})$.

CONCLUSION

NanoZSM-5 was synthesized with crystal size ≤ 30 nm by using an interrupted ultrasound crystallization process. In this process, the hydrothermal treatment was interrupted with ultrasound and without ultrasound at 170 °C for 24 hours. The nanoZSM-5 crystallinity was confirmed by X-ray diffraction. The crystallite size and morphology were determined by HRTEM whilst ^{29}Si MAS NMR confirmed the framework composition and presence of silanol group

at the surface of the nanoZSM-5.

A mechanism to rationalise the effect of interrupted ultrasound to enhance the formation of nanoZSM-5 is also proposed. It is based on the influence of cavity generation of ultrasound to assist the nucleation and growth steps to facilitate the synthesis of nanostructured ZSM-5 zeolite.

Acknowledgements

The authors are thankful to the included universities for their technical and financial cooperation.

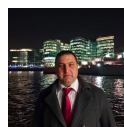
Bibliography

- Moliner M. Direct Synthesis of Functional Zeolitic Materials. ISRN Mater Sci. 2012;2012:1–24.
- Gobbi C. No Title. 1985;89:1070–2.
- Hay DG, Jaeger H, West GW. the Monoclinic-Orthorhombic Transition in Silicallte Using XRD and Silicon NMR. J Phys Chem. 1985;89(1979):1070–2.
- Tago T, Konno H, Sakamoto M, Nakasaka Y, Masuda T. Selective synthesis for light olefins from acetone over ZSM-5 zeolites with nano- and macro-crystal sizes. Appl Catal A Gen. 2011;403(1–2):183–91.
- Jiri C, Avelino C. Zeolites and catalysis Synthesis, Reaction and Application. 1st ed. Weinheim: Wiley-VCH; 2010. 882 p.
- Fraenkel D, Cherniavsky M, Ittah B, Levy M. Shape-selective alkylation of naphthalene and methylnaphthalene with methanol over H-ZSM-5 zeolite catalysts. J Catal. 1986;101(2):273–83.
- Jin Y, Li Y, Zhao S, Lv Z, Wang Q, Liu X, et al. Synthesis of mesoporous MOR materials by varying temperature crystallizations and combining ternary organic templates. Microporous Mesoporous Mater. 2012;147(1):259–66.
- Van Der Gaag FJ. ZSM-5 type zeolites: Synthesis and use in gasphase reactions with ammonia. Delft University Press; 1987. 1–132 p.
- Iwakai K, Tago T, Konno H, Nakasaka Y, Masuda T. Preparation of nano-crystalline MFI zeolite via hydrothermal synthesis in water/surfactant/organic solvent using fumed silica as the Si source. Microporous Mesoporous Mater. 2011;141(1–3):167–74.
- Pu S-B, Inui T. 7. Zeolites. 1996;17:334–9.
- Adeyuyi YG, Klocke DJ, Buchanan JS. Effects of high-level additions of ZSM-5 to a fluid catalytic cracking (FCC) RE-USY catalyst. Appl Catal A, Gen. 1995;131(1):121–33.
- Tosheva L, Valtchev VP. Nanozeolites: Synthesis, crystallization mechanism, and applications. Chem Mater. 2005;17:2494–513.
- Grieken R V., Sotelo JM, Melero JA. Anomalous crystallization mechanism in the synthesis of nanocrystalline ZSM-5. Microporous Mesoporous Mater. 2000;39:135–47.

14. Guo Z, Jones AG, Li N. The effect of ultrasound on the homogeneous nucleation of BaSO₄ during reactive crystallization. *Chem Eng Sci.* 2006;61(5):1617–26.
15. Epping JD, Chmelka BF. Nucleation and growth of zeolites and inorganic mesoporous solids: Molecular insights from magnetic resonance spectroscopy. *Curr Opin Colloid Interface Sci.* 2006;11(2–3):81–117.
16. Vafaeian Y, Haghghi M, Aghamohammadi S. Ultrasound assisted dispersion of different amount of Ni over ZSM-5 used as nanostructured catalyst for hydrogen production via CO₂ reforming of methane. *Energy Convers Manag.* 2013;76:1093–103.
17. Askari S, Miar Alipour S, Halladj R, Davood Abadi Farahani MH. Effects of ultrasound on the synthesis of zeolites: A review. *J Porous Mater.* 2013;20(1):285–302.
18. Krishnakumar V. *Crystal Growth Introduction.* 2014.
19. Verdager SV. Synthesis in solution [Internet]. Instituto de Ciencia de Materiales de Madrid. Available from: http://www.icmm.csic.es/csc/?page_id=172
20. Sharma P, Yeo J, Han MH, Cho CH. NaA zeolite cubic crystal formation and deformation: cubes with crystalline core, simultaneous growth of surface and core crystals, and layer-by-layer destruction. *RSC Adv.* 2012;2(20):7809.
21. Abrishamkar M, Azizi SN, Kazemian H. Ultrasonic-assistance and aging time effects on the zeolite process of BZSM-5 zeolite. *Zeitschrift für Anorg und Allg Chemie.* 2010;636(15):2686–90.
22. Nicolaidis CP, Kung HH, Makgoba NP, Sincadu NP, Scurrill MS. Characterization by ammonia adsorption microcalorimetry of substantially amorphous or partially crystalline ZSM-5 materials and correlation with catalytic activity. *Appl Catal A Gen.* 2002;223(1–2):29–33.
23. Triantafyllidis KS, Nalbandian L, Trikalitis PN, Ladavos AK, Mavromoustakos T, Nicolaidis CP. 10. *Microporous Mesoporous Mater.* 2004;75(1–2):89–100.
24. Hsu CY, Chiang AST, Selvin R, Thompson RW. Rapid synthesis of MFI zeolite nanocrystals. *J Phys Chem B.* 2005;109(40):18804–14.
25. Pan F, Lu X, Zhu Q, Zhang Z, Yan Y, Wang T, et al. A fast route for synthesizing nano-sized ZSM-5 aggregates. *J Mater Chem A.* 2014;2(48):20667–75.
26. Schmidt I, Madsen C, Jacobsen CJH. Confined space synthesis. A novel route to nanosized zeolites. *Inorg Chem.* 2000;39:2279–83.
27. Guo Z, Jones a. G, Li N. The effect of ultrasound on the homogeneous nucleation of BaSO₄ during reactive crystallization. *Chem Eng Sci.* 2006;61(5):1617–26.
28. Musyoka NM, Petrik LF, Hums E. Ultrasonic assisted synthesis of zeolite A from coal fly ash using mine waters (acid mine drainage and circumneutral mine water) as a substitute for ultra pure water. *Imwa.* 2011;423–8.
29. IChemE. 14th international symposium on industrial crystallization. In: 14th international symposium on industrial crystallization. 1999. p. 200.
30. Venkathri N. synthesis and characterization of a microcrystalline ZSM-5 melcualr sieve. *React Kinet CatalLett.* 2007;91:283–9.
31. Awala H, Gilson J-P, Retoux R, Boullay P, Goupil J-M, Valtchev V, et al. Template-free nanosized faujasite-type zeolites. *Nat Mater.* 2015;14(4):447–51.
32. Majano G, Darwiche A, Mintova S, Valtchev V. Seed-induced crystallization of nanosized Na-ZSM-5 crystals. *Ind Eng Chem Res.* 2009;48(15):7084–91.
33. Mintova S, Valtchev V. Effect of the silica source on the formation of nanosized silicalite-1: an in situ dynamic light scattering study. *Microporous Mesoporous Mater.* 2002;55(2):171–9.
34. Moreno-Piraján JC, Garcia-Cuello VS, Giraldo L. Synthesis of HMOR and HZSM-5 and their Behaviour in the Catalytic Conversion of Methanol to Propylene (MTP). *J Thermodyn Catal.* 2010;01(01):1–8.
35. Wenyang X, Jianquan L, Wenyuan L, Huiming Z, Bingchang L. Nonaqueous synthesis of ZSM-35 and ZSM-5. *Zeolites.* 1989;9(6):468–73.
36. Sklenak S, Dědeček J, Li C, Wichterlová B, Gábová V, Sierka M, et al. Aluminium siting in the ZSM-5 framework by combination of high resolution 27Al NMR and DFT/MM calculations. *Phys Chem Chem Phys.* 2009;11(8):1237–47.
37. Zhang W, Bao X, Guo X, Wang X. A high-resolution solid-state NMR study on nano-structured HZSM-5 zeolite. 1999;60:89–94.
38. Jacobsen CJH, Madsen C, Janssens TVW, Jakobsen HJ, Skibsted J. Zeolites by confined space synthesis - characterization of the acid sites in nanosized ZSM-5 by ammonia desorption and 27Al/29Si-MAS NMR spectroscopy. *Microporous Mesoporous Mater.* 2000;39:393–401.
39. Klinowski J. Recent Advances in Solid-State NMR of Zeolites. *Annu Rev Mater Sci.* 1988;18(1):189–218.

Affiliations and Corresponding Informations

Corresponding: Farrukh Arsalan Siddiqui
 Email: farrukh.siddiqui@bzu.edu.pk
 Phone:



Pirzada Afridi:



Farrukh Arsalan Siddiqui:

Department of Mechanical Engineering, Bahauddin Zakariya University, Multan, Pakistan



Sergio Gonzalez-Cortes:

Inorganic Chemistry Laboratory, South Park Road, OX1 3QR, Oxford University, Oxford, UK



Liam France:

Inorganic Chemistry Laboratory, South Park Road, OX1 3QR, Oxford University, Oxford, UK